

## ARTICLE OPEN



# Fire-retardant effect of titania-polyurea coating and additional enhancement via aromatic diamine and modified melamine polyphosphate

Ze Rong<sup>1,7</sup>, Yuanzhe Li<sup>2,7,8✉</sup>, Rachel ZhiQi Lim<sup>2</sup>, Haojing Wang<sup>3</sup>, ZhiLi Dong<sup>2,8</sup>, Kexin Li<sup>4</sup> and Xueli Wang<sup>5,6</sup>

Polymeric materials and composites are well suited to support structures in marine conditions due to their corrosion resistance. However, their low glass transition temperature makes them vulnerable to softening at high temperatures. Hence, fire retardancy is a key aspect if these materials are selected to ensure stiffness under flammable conditions. In this paper, a fire-retardant polyurea coating for industrial applications is proposed. The aromatic diamine and aliphatic diisocyanate are believed to have a synergistic effect in improving flame properties. Moreover, various combinations of flame-retardant additives with aromatic and aliphatic-based polyurea are mixed to further improve fire-retardancy. Through the characterizations of their glass transition temperature and delay in the ignition, it indicates that the combination of Talc and melamine polyphosphate may provide an outstanding enhancement for the Titania-polyurea coating, and such enhancement may improve its original tensile and compression strength, and surface hardness as well.

*npj Materials Degradation* (2022)6:38; <https://doi.org/10.1038/s41529-022-00248-y>

## INTRODUCTION

Fire-retardant coatings are often required to protect a wide range of products both flammable and non-flammable against fire. It is the oldest, most efficient, and easiest method to apply to any surface without modifying the intrinsic properties of materials<sup>1</sup>. The degree of fire retardation mainly depends on the coating thickness, substrates, and efficiency of formulations. Fire-retardants (FRs) are supposed to be added to the coating system to reduce its flammability<sup>2</sup>. Unfortunately, no single FR has been shown to provide effective flame retardation and low smoke evolution in previous research on polyurethane (PU) as well as PUA. Normally 20–30% by weight of FRs are supposed to add for effective flame resistance or fire retardancy, whereas in the case of mineral fillers, more than 60% is needed. These pre-requisites are very likely to have a detrimental effect on processing and may also reduce mechanical properties<sup>3</sup>. To overcome these disadvantages, a combination of FRs with polyurea coating is utilized for effective flammability reduction, decreased smoke production, as well as ensuring a minimal loss of physico-mechanical properties.

Polyurea (PUA) coating has received attention as a protective surface coating due to its characteristics such as fast setting, solvent-free, resistance to a broad range of corrosives and solvents, good thermomechanical properties, adhesion, and anti-abrasive properties. In previous research, a Titania-polyurea spray antibacterial coating has been fabricated, and such coating is able to prevent biofilm and bacteria from enriching on the surface and reduce the growth of mold effectively. It can utilize oxygen radicals generated to inhibit the growth of various microorganisms or to destroy the cell structures of the microorganisms<sup>4</sup>. Despite many outstanding qualities, the efficacy of traditional polyurea (PUA) coating may be limited in many applications due

to relatively low flammability and the release of toxic smoke while burning. Moreover, its wider applications in marine, as well as some special surfaces through additional enhancement, have been further considered. Fire-retardants shall be selected and added as the additional enhancement to polyurea coating to prevent fires from starting, limit the spread of fire, and minimize fire damage. Some fire-retardants may work effectively on their own, while others may act as a synergist to increase the fire protection benefits of other fire retardants<sup>5</sup>. The type of fire-retardants may vary depending on the component of polyurea backbones according to their physical nature and chemical composition. Hence, fire-retardants must be matched appropriately to the different types of polyurea backbones as well as any other components. However, the reviews or any study related to fire-retardant modifications of polyurea coating series have been seldom documented<sup>6</sup>.

Generally, brominated compounds and chlorinated organic compounds are used because iodides are thermally unstable at processing temperature and the effectiveness of fluorides is low. The behavior of these halogenated fire retardants in processing conditions and their effect on properties and the long-term stability of the resulting material are among the criteria that must be considered. Moreover, it is particularly recommended to use an additive that produces halide to the flame at the same range of temperature of polymer degradation into combustible volatile products<sup>7–9</sup>. However, the biggest problem for these halogenated FR compounds should be the environmental issue, such as generating toxic gas and substance may generate after burning. Other than these halogenated compounds, one recent research done by Arkunkumar T has been looking into using polymer-based FRs to improve damage control materials to address fire

<sup>1</sup>School of Mathematical and Physical Sciences, University College London, London WC1E 6BT, United Kingdom. <sup>2</sup>School of Materials Science & Engineering, Nanyang Technological University, Singapore 639798, Singapore. <sup>3</sup>School of Chemical and Biomedical Engineering Nanyang Technological University, Singapore 639798, Singapore. <sup>4</sup>Hwa Chong International School, Singapore 269783, Singapore. <sup>5</sup>Institute of Central China Development, Wuhan University, Wuhan 430072, People's Republic of China. <sup>6</sup>Department of Geography, National University of Singapore, 1 Arts Link, 117570 Singapore, Singapore. <sup>7</sup>These authors contributed equally: Ze Rong, Yuanzhe Li. <sup>8</sup>These authors jointly supervised this work: Yuanzhe Li, and ZhiLi Dong. ✉email: yuanzhe001@e.ntu.edu.sg

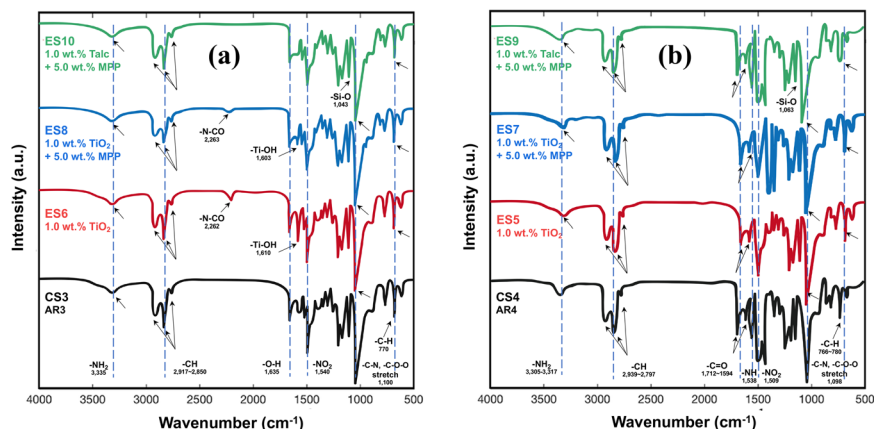


**Fig. 1** FTIR spectrum of coating samples **a** AR3 matrix (IPDI base) series with aromatic diamine only and **b** AR4 matrix series (MDI base) with both aromatic diamine and aromatic diisocyanate.

mitigation of polyurethane (PU)<sup>10</sup>. To ensure that the effectiveness of polyurethane (PU) is able to meet the fire-mitigation properties, an investigation of non-halogenated additives, melamine polyphosphate (MPP), has been carried out<sup>10,11</sup>. All the coating samples at the start indicated some similar characteristics like no charring and dripping. For MPP-blended PU, a decrease in heat release rate (HRR) was observed which can be a result of a synergistic effect between the FR additives<sup>11</sup>. During the limiting oxygen test, all the samples have anxious properties such as severe shrinkage, erratic burning, dripping, no charring, and afterglow. The result also shows that the addition of MPP does not influence the smoke discharge while burning. The results indicate that the 10% and above quantities of MPP with PU have significant fire retardancy and smoke suppression efficiency, and such results may also lead to the interest in polyurea<sup>10–12</sup>.

In this study, the fire-retardant effect of Titania-polyurea coatings in flammability and heat resistance has been identified. Several methods are explored in efforts to improve the fire retardancy and resistance of polyurea and Titania-polyurea coatings. This project aims to formulate an appropriate combination of fire-retardant polyurea coating. The proposed approach may include the chemical incorporation of fire-retardant additives into the molecular structure of the polyurea, the mechanical incorporation of fire-retardant fillers as well as polyurea-backbone substitution. The performances of fire protection, mechanical, chemical, and physical properties of flame-retardant coatings are also evaluated and investigated within the tests. The properties are to be evaluated based on time to ignition, smoke generation, and char stability. Though the aspect of functionalization and application of polyurea coatings is still in the early stages, in the near future, more and more interesting materials based on PUA will be successfully developed for the incorporation into coatings.

## RESULTS AND DISCUSSION

### Fourier transform infrared (FTIR) spectroscopy results

The synthesis of the polyurea coating with aromatic-substitute (MDI) and isophorone diisocyanate (IPDI) series backbones and modifications of fire-retardant additives via TiO<sub>2</sub>, Talc, and MPP was confirmed by comparing their Fourier transform infrared (FTIR) spectrum, as shown in Fig. 1. For the basic polyurea-backbone group, CS3 and CS4, the most important bands were the ones resulting from the vibration of N–H and C=O bonds, representing the urea linkage. In the bottom of FTIR spectra of Fig. 1a, b, the bands observed around 1712 cm<sup>-1</sup> were related to the stretching of the carbonyl group, corresponding to the hydrogen-bonded to the carbonyl group. The broadband at 3335 cm<sup>-1</sup> and 3350 cm<sup>-1</sup> respectively in CS3 and CS4 were related to stretching

of N–H in particular to the secondary amines from Versalink<sup>®</sup> P1000 and the strong band at 1540 cm<sup>-1</sup> was related to the vibration of the –NO<sub>2</sub> bond from the urea linkage, directly connected to the carbonyl group<sup>13,14</sup>. In Fig. 1b, the band presented at 2262 cm<sup>-1</sup> corresponded to the stretching vibration of the N–CO bond, probably due to unpolymerized residues from the diisocyanate (IPDI) that was not fully consumed<sup>15</sup>.

Besides, FTIR spectroscopy was also a powerful tool for the identification of polysaccharides in the MPP, which might also provide valuable information for further structural study on MPP. As shown in Fig. 1a, and similarly in Fig. 1b, there were two characteristic absorptions bands of polysaccharides: a strong and wide absorption band at about 3307 cm<sup>-1</sup> and 3338 cm<sup>-1</sup> for O–H stretching vibration, and a band in the region of 2939 cm<sup>-1</sup> and 2943 cm<sup>-1</sup> for C–H stretching vibration, respectively found in the IR spectrum of ES7 and ES8. The band at about 1099 cm<sup>-1</sup> and 1100 cm<sup>-1</sup> respectively in ES7 and ES8 were assigned to the valent vibrations of the C–O–C bond and glycosidic bridge<sup>4,15</sup>. The characteristic absorptions at around 854 cm<sup>-1</sup> indicated that  $\alpha$ - and  $\beta$ -configurations of the sugar units might simultaneously exist in MPP. However, as the introduction and increment of a small weight amount of fire retardants, TiO<sub>2</sub> and Talc, the peak of the original polyurea was slightly transformed, and some of the small peaks might be squeezed together to a bigger one, which was due to the distribution of these hard segments inside the polyurea coatings. Still, the Ti–OH bond from TiO<sub>2</sub> as well as Si–O bond from Talc powder could be observed at 1603 cm<sup>-1</sup> to 1610 cm<sup>-1</sup> and 1043 cm<sup>-1</sup> to 1063 cm<sup>-1</sup> respectively after confirmed with the literatures<sup>13</sup>.

### Transmission electron microscopy (TEM)

Figure 2 depicted the correspondent transmission electron microscopy (TEM) imaging of polyurea coatings with titanium dioxide and Talc (Mg<sub>3</sub>Si<sub>4</sub>O<sub>10</sub>(OH)<sub>2</sub>). In the case of coating sample ES7 (Fig. 2a, b), the TiO<sub>2</sub> platelet with a tetragonal or similar crystal structure was able to be observed clearly. While in the case of coating sample ES9 (Fig. 2c, d), the Talc powder with more complex trioctahedral and dioctahedral structures could be observed. Such observations were in accord with the TEM imaging of titanium dioxide and Talc as illustrated in the literature citations<sup>7,9,14</sup>. Besides, all the TEM images for these fire-retardant polyurea coatings with FR additives, including TiO<sub>2</sub>, Talc, and MPP, revealed similar micro-structures as the ones with ES7 and ES9. Although the coating samples were not fully transparent even with less containing the FRs, the well distributions for all the fire retardants (FRs) in the polyurea matrix could be demonstrated rather than agglomeration<sup>13</sup>. The boundary of both samples was

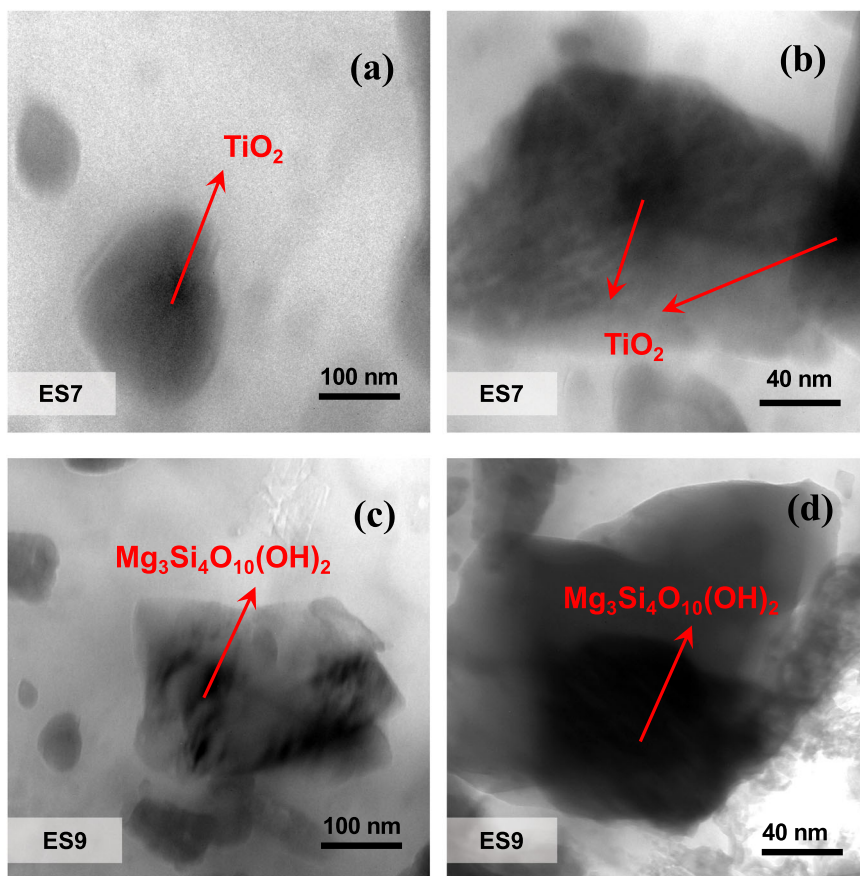


**Fig. 2** TEM images of polyurea coatings with **a, b** ES7 coating sample with  $\text{TiO}_2$  + MPP and **c, d** ES9 sample with Talc + MPP.

blurred, which was supposed to be the MPP shell packing these inorganic hard segments. The imaging of coating sample ES7 groups in Fig. 2a, b also indicated the simple crystal structures of titanium dioxide within the polyurea coating matrix, which could be correlated to the monoclinic crystal structure of the titanium oxide.

#### Effects of fire retardants loading on physico-mechanical properties of polyurea

The physico-mechanical properties of fire-retardant polyurea are important parameters that determine its applications, as lower mechanical properties mean the materials being more susceptible to destruction by outside forces. All tensile and compression strength and surface hardness results were listed in Table 1, and the aromatic diamine groups (CS3 and CS4) had a significant increase compared with the normal diamine ones (CS1 and CS2). The higher the failure strain, the better the crack resistance of the coating when the substrate was bent. The tensile test results showed that at a high strain rate, which was set as high as 500%, the test specimens did not exhibit obvious fracture. After a continuous increase in the strain rate up to around 750%, initial microcracks happened and then most of the specimens fractured into several pieces shortly. It indicated that the AR4 matrix series (MDI-based) had a slightly higher tensile strength than AR3 matrix ones (IPDI) even with the same FR additives, which might be due to the introduction of more aromatic function groups. The fracture surfaces of specimens with  $\text{TiO}_2$  and Talc in creep and quasi-static tensile tests were relatively rough. However, the addition of MPP exhibited some extended binder filaments bridging the crack surfaces, demonstrating that the MPP within the polyurea coatings might also serve as a binding agent also to retain its

**Table 1.** Effect of flame-retardant loading on physico-mechanical properties of polyurea.

Formula no.	Tensile strength/MPa	Compression stress/MPa	Shore hardness/A
CS1	8.5	16.5	39
CS2	9.3	18.6	41
CS3	10.8	26.2	38
CS4	10.5	24.8	36
ES5	17.6	24.4	43
ES6	16.9	34.6	58
ES7	17.3	26.8	50
ES8	16.2	28.6	49
ES9	15.7	30.8	51
ES10	12.6	24.2	47

integrity and underwent considerable deformation when the tensile stress acted. Compression test results showed that the compression stress of  $\text{TiO}_2$  were higher than the same matrix coating group of Talc. ES6 with  $\text{TiO}_2$  only had the highest yield stress at 34.6 MPa. The introduction of the MPP might low down the compression strength but increase the flexural strength. No significant yield stress was found in the compression test for all groups of coating specimens. The hardness results revealed that the CS3, which was the control group with IPDI as the isocyanate base and P1000 as the diamine base, had a slightly higher hardness value compared to CS4, which is the control sample with MDI as the isocyanate base. Based on the hardness test results, the

addition of  $\text{TiO}_2$  increases the hardness value for IPDI-based samples, while it decreased the hardness value for MDI-based samples. This trend was seen for the addition of MPP and  $\text{TiO}_2$  as well as shown in ES7 and ES8. In specimen groups, ES9 and ES10, the addition of Talc and MPP also increased the hardness value for MDI as well as IPDI. And this hardness test result was also consistent with the compression behavior mentioned above. Overall, the ES6 specimen group with AR3 matrix (IPDI-based) coatings had the most average physico-mechanical behaviors among all the specimens. Followed by the ES7 specimen group with AR4 matrix (MDI-based), both experimental groups without MPP indicated a slightly better performance in one or two of the mechanical aspects. These physico-mechanical properties might also become a great reference for the optimization works for the formula design.

### Differential scanning calorimetry (DSC) results

The investigation of thermodynamic properties of polyurea samples systems was conducted for both AR3 matrix (IPDI base) polyurea coating samples and AR4 matrix (MDI base) coating samples using differential scanning calorimetry. It is an important method to study the aggregative states and thermal transformation of polyurea as well as any other polymer materials. The DSC results were shown in Fig. 3a, b, and the glass transition of a soft segment for the first heating scans of all the coating samples was marked in the figures. As softening temperature since  $T_g$  was much lower than melting temperature, hence, the glass transition, also considered as melting point ( $T_m$ ), of each polyurea coating group was necessary to study<sup>16</sup>. As illustrated in Fig. 3, with the temperature increasing, these coating samples indicated their endothermic peaks within the range of 110 to 190 °C. The melting range of each curve was long and the shape of each peak was not

sharp, which might be caused by the separation structures of fire retardants (FRs). And further observations of the melting would be also obtained via scanning electron microscopy (SEM) after the flammability test. The results for both AR3 and AR4 matrixes showed minor loss as low as 17% in weight. From the horizontal comparisons of Fig. 3a, b, it could be observed that the polyurea with a more aromatic-substituted backbone would have higher hard segment crystallinity and better thermal stability compared to the aliphatic backbone. The main reason might be due to the introduction of aromatic diamine, which contains side nitrogen groups, would increase the random copolymerization of the polyurea coatings<sup>17,18</sup>.

Whereas from the vertical comparison within Fig. 3a, b, the melting point ( $T_m$ ) slightly decreased with the add-on of MPP in the Titania-Polyurea coating samples. The contributing factor might be the large side-chain structure of MPP, which might reduce the random copolymerization of polyurea. However, as the temperature continuously went up, DSC curves should reveal a higher degree of the hard segment ordering exhibited by the presence of endothermic peaks, which should be dominated by those FRs. Besides, the polyurea coating groups with MPP would indicate a higher second endothermic peak, which was believed to be caused by the shell structure between MPP and  $\text{TiO}_2$ . To sum up, MPP could enhance the thermodynamic properties of  $\text{TiO}_2$  and indicate better compatibility in MDI-based polyurea, whereas MPP could enhance the thermodynamic effect of IPDI-based polyurea as well, but it would only indicate well compatibility with Talc.

### Flammability test results

Figure 4 demonstrated the setup for the flammability test, which included the burning from two-dimension. Such a flammability test was to find out the flammability of polyurea by testing on a stripe

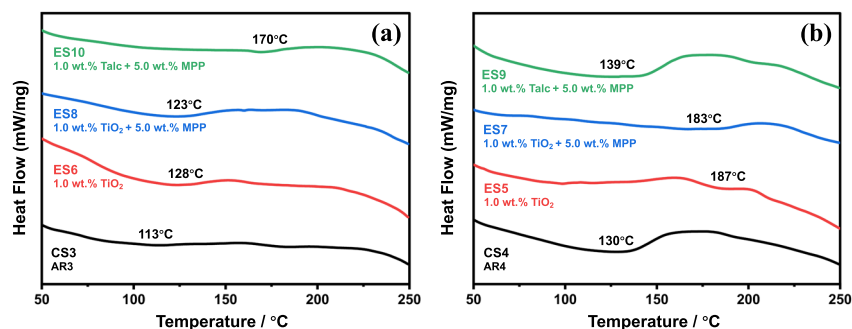


**Fig. 3** DSC curves of coating samples **a** AR3 series with aromatic diamine only and **b** AR4 series with both aromatic diamine and aromatic diisocyanate.

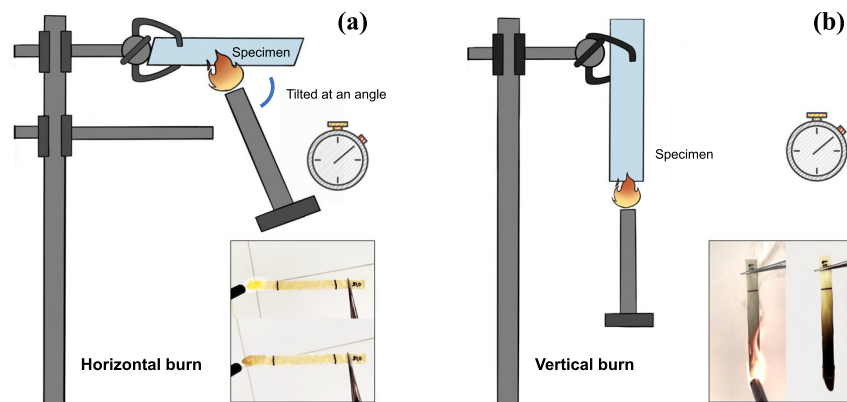


**Fig. 4** Flammability test setup **a** horizontal burn and **b** vertical burn of polyurea coating according to ASTM D635 standard.



**Table 2.** Flammability test results of coating samples.

Formula no.	Time to ignition (horizontal)/t (secs)	Horizontal burn elapsed time/t (secs)	Time to ignition (vertical)/t (secs)	Vertical burn elapsed time/t (secs)	Smoke emission/flaming drips	Observation
CS1	1	Cannot self-elapsed	1	Cannot self-elapsed	Thin smoke/ Continuous drips	High flammability with dark char.
CS2	2	Cannot self-elapsed	1	Cannot self-elapsed	Thin smoke/ Continuous drips	Moderate flammability with dark char.
CS3	5	5	4	9	— / —	Form an insulating layer and shape slightly changed.
CS4	3	3	4	10	Thin smoke/ —	Form a slight char and volume slightly decreased.
ES5	— (No flame)	0	No flame	0	— / 1–2 drips	Form char within the first column.
ES6	5	15	3	8	— / 4–5 rips	Form a thick insulating layer, burn to the second column, and shape significantly changed.
ES7	— (No flame)	0	11	4	— / —	Form slight char and maintain its shape.
ES8	3	10	2	8	— / 2–3 drips	Form an insulating layer and shape moderately changed.
ES9	8	8	6	12	Heavy smoke / —	Form very dark char and burn passed to the last column.
ES10	4	8	No flame	0	— / —	Maintain its shape.

of the samples cut to the same dimensions and was tabulated<sup>17,18</sup>. Both horizontal and vertical burn would serve to verify the uniform distribution and the identification of the fire-retardancy for the polyurea coating. From the flammability test results as summarized in Table 2, failure polyurea specimen groups, CS1 and CS2, were considered as a flammable, the other two groups of polyurea specimen groups, CS3 and CS4, might also form a slight char, shape all got slightly deformed, and ignition time was considered as short as combustible substance. Whereas the polyurea coating samples with the addition of FR additives all performed well in the flammability test only except ES9. This might be due to plenty of carbon present in the polymer sample to form char<sup>19</sup>. Char was known to act as a barrier between the fire and polymers, however, it burned passed the mark making it flammable unlike the rest of the samples which were self-extinguishing. This observation was also consistent with the finding in the DSC curves in Fig. 3b.

The cracks, void, and bubbles as shown in Fig. 5 were majorly caused by the high-temperature exposure and the softening of the polyurea backbones, which were common in most of the flammability test for polymer coatings. After the polyurea was mixed with fire retardants (FRs), it did not propagate its flammability property. The time to ignition was also prolonged, ES5 and ES7 specimens even would not catch fire with enough time of ignition. Although flaming drips and smoke emissions were found in some of the specimens, polyurea coating with FRs were still able to elapse themselves. And most of the specimens would not generate char after burning. The AR3 series (IPDI base) polyurea coating in Fig. 5a had the less char length compared with the similar FR additives groups in the AR4 series (MDI base) indicated in the right, while most of the AR3 series (left) failed to maintain its original shapes than AR4 series would perform in the flammability test. The same observation could also be observed in SEM images (Fig. 6) in the left slide of the cross-section of the unburnt and burnt polyurea in flammability tests. The ES10 of the AR3 series indicated a good combination among the IPDI-based polyurea matrix, Talc, and MPP, whereas the interface with maintained shapes among IPDI-based polyurea matrix, TiO<sub>2</sub>, and MPP (ES6 and ES8) was relatively poor and might cause serious damage of the composite internal structure, ending up with the deformation of its external configuration<sup>20</sup>. On the right side of Figs. 5, 6, a better combination between MDI-based polyurea matrix and TiO<sub>2</sub> could be observed. Both ES5 and ES7 indicated relatively uniform micro- and macro-structures before and after the flammability test. After burning, at 350x magnification SEM images of ES5 and ES7, dense and compact microstructure between TiO<sub>2</sub> and MDI-based polyurea matrix remained, which indicated better fire-retardant performance, whereas the Talc and MDI-based polyurea matrix (ES9) demonstrated relatively poor compatibility with poor flammability test where a burned black char region char was formed, and the burn passed to the last column.

The above scenarios clearly stated that with proper FR additives in the polyurea coatings, e.g., TiO<sub>2</sub>, Talc, and MPP, polyurea coatings might become a totally self-extinguishing material and strongly crossed out the flammable characteristics of polyurea, which made it more reliable for practical applications. Among all the experimental groups, ES10 gave the best result, and it was believed to be the combination of aliphatic diisocyanate, aromatic diamine, MPP, and Talc that stabilized the layer and kept the surface from further burning<sup>21</sup>. Moreover, the addition of TiO<sub>2</sub> and MPP also indicated an outstanding fire-retardant property on its heel with a slight char only on the surface after burning and a high melting point ( $T_m$ ) in previous DSC curves.

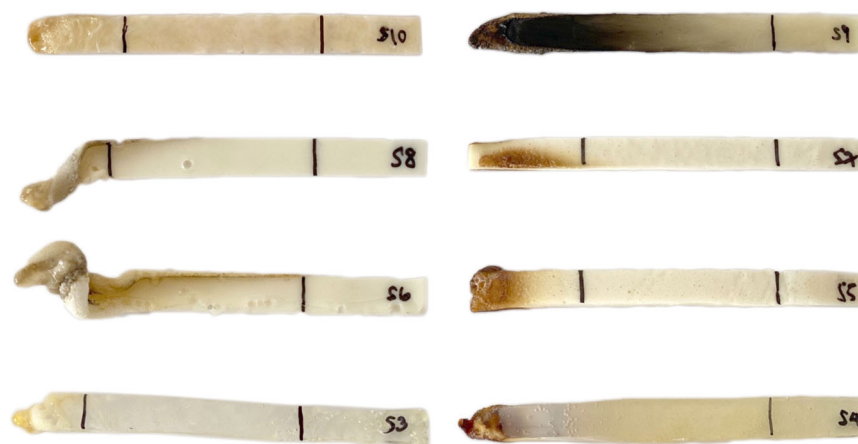


**Fig. 5** Flammability property of coating samples. **Left:** AR3 series with aromatic diamine only. **Right:** AR4 series with both aromatic diamine and aromatic diisocyanate after flammability test.

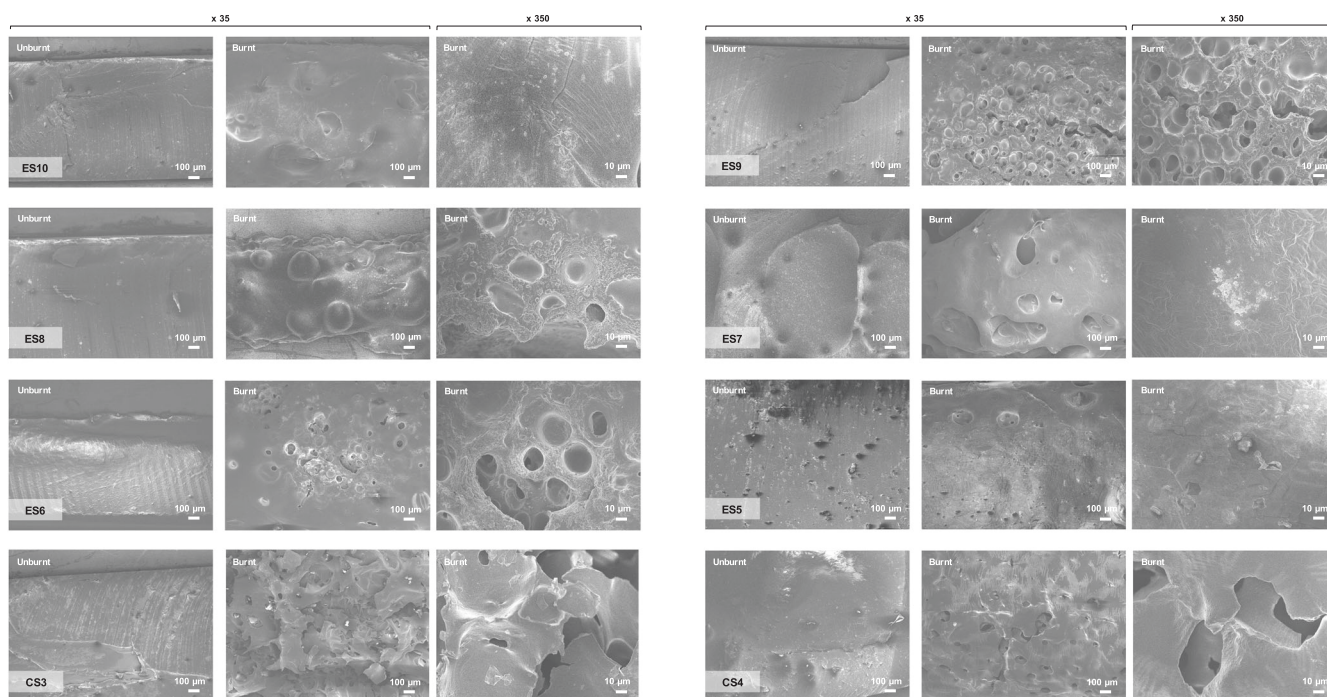


**Fig. 6** SEM micrographs of the cross-section of the unburnt and burnt polyurea in flammability tests. **Left:** AR3 series with aromatic diamine only. **Right:** AR4 series with both aromatic diamine and aromatic diisocyanate.

### Melamine polyphosphate (MPP) fire-retardant mechanism of action

Moreover, through the upper SEM images (Fig. 6) of the cross-sections of the unburnt and burnt polyurea coating samples with MPP in flammability tests, it could be observed that the MPP could retard ignition by causing a heat sink through endothermic dissociation followed by endothermic sublimation of the melamine itself at its melting temperature (Fig. 7). Additionally, a larger heat sink effect might be generated by the subsequent decomposition of the melamine vapors<sup>10,21</sup>. Comparing the flammability test results and SEM images, the mechanism could be hypothesized that MPP regarded as a poor fuel would have a heat of combustion of only 40% of that of hydrocarbons. Furthermore, the nitrogen produced by combustion would possibly act as an inert diluent. Another source of inert diluent was the ammonia which was released during the breakdown of

the melamine or self-condensation of the melamine fraction which did not sublimate<sup>8,9,22</sup>.

MPP could also show a considerable contribution to the formation of a char layer in the intumescent process. The char layer acted as a barrier between oxygen and polymeric decomposition gases. Char stability was enhanced by multi-ring structures like melem and melon, formed during self-condensation of melamine. In combination with phosphorous synergists melamine could further increase char stability through the formation of nitrogen-phosphorous substances. Furthermore, MPP could also act as a blowing agent for the char, enhancing the heat barrier functionality of the char layer<sup>7–10</sup>.

Melamine-based flame retardants only represent a small but fast-growing segment in the flame-retardant family. Melamine-based flame retardants demonstrate flame-retardant properties and versatility in polyurea coating because of their abilities to employ various modes of flame-retardant actions<sup>6</sup>. These actions

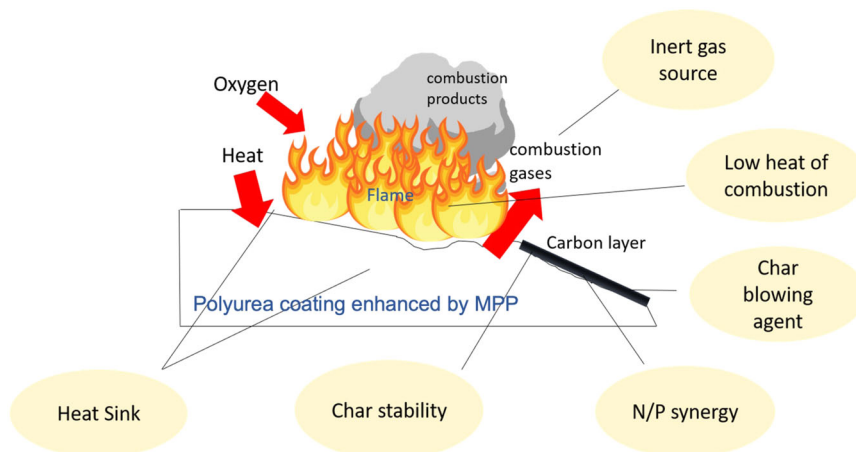


**Fig. 7** Melamine-based fire-retardant combustion stages.

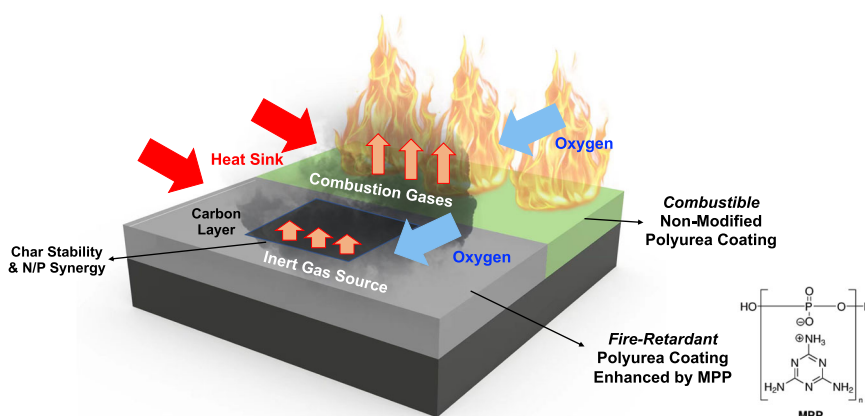


**Fig. 8** Fire flammability comparison between combustible non-modified polyurea coating and fire-retardant polyurea coating enhanced by MPP.

include chemical interference, heat sink, char formation, intumescence, inert gas, and heat transfer (dripping). In this family of non-halogenated flame retardants, three chemical groups can be distinguished: (i) Pure melamine; (ii) Melamine derivatives, e.g., salts with organic or inorganic acids such as boric acid, cyanuric acid, phosphoric acid, or pyro/poly-phosphoric acid, and (iii) Melamine homologs such as melam, melem, and melon. Flame retardants function by interference with one of the three components that initiate and/or support combustion: heat, fuel, and oxygen<sup>7–9</sup>. Melamine shows a flame-retardant effect because of its ability to interfere with the combustion process in all stages.

In summary, it is illustrated that polyurea as an individual material is considered flammable or combustible, but with the addition of fillers and additives, the fire-retardant property can be achieved (Fig. 8). The basic flammability test explored that substituting the isocyanate backbone from diisocyanate polyurea backbone to isophorone diisocyanate or modification of the normal diamine with aromatic diamine can significantly improve their fire-retardant properties. Backbone matrix composed of MDI and IPDI isocyanate and aromatic diamine were the optimized formula group to have better fire-retardant than with normal diamine, and such optimized group may also improve the tensile and compression strength, and surface hardness of the polyurea coatings. It has been shown that these organic rings from aromatic diamine increase the formation of the char layer which in turn lowers the heat release rate. This work further explored the

use of flame-retardant fillers and additives to enhance the flammability properties of polyurea. The top two fire-retardant coating coatings were observed with the additional additives of Talc and MPP or TiO<sub>2</sub> and MPP. In combination with synergists such as melamine polyphosphate (MPP), stable chars were achieved. The addition of fire-retardant additives and fillers has also shown to have no major impact on its mechanical properties, and some even have better surface morphology, higher glass transition temperature at around 190 °C, and longer delay time in the ignition, with no significant char or flame. In future work, the explosive test of such polyurea coatings shall be explored for more military applications.

## METHODS

### Materials

About 50–80 wt% isophorone diisocyanate (IPDI)—Component A and 50–90 wt% poly (propylene glycol) bis (2-aminopropyl ether) (Jeffamine® D400)—Component B were obtained from Sigma-Aldrich and Huntsman (Bangkok, Thailand), respectively. The aromatic-substitute (MDI) in the diisocyanate portion (Aromatic Component A) used in this experiment was commercially purchased from Dow Chemical Company. The aromatic-substitute in the diamine portion (Aromatic Component B) was prepared by reacting 30% Ethacure® 300 with 70% Versalink® P1000. Fire-retardant (FR) chemicals melamine polyphosphate (MPP, Foshan, China), nano-titanium dioxide (TiO<sub>2</sub>, Sigma-Aldrich, Bangkok, Thailand), and clay mineral, composed of hydrated magnesium silicate with the chemical formula



Mg<sub>3</sub>Si<sub>4</sub>O<sub>10</sub>(OH)<sub>2</sub> (Talc, Sigma-Aldrich, Bangkok, Thailand) were used as provided.

### Synthesis of aromatic backbone polyurea

For the fabrication of aromatic backbone polyurea, 50 wt% Component A and 50 wt% Component B of the basic polyurea formulation (AR1) were systematically replaced with the aromatic amines as described in Supplementary Table 1 (AR2 and AR3). To make a comparison, another polyurea formulation would be examined between Component A/B and aromatic diisocyanate/diamine (AR4).

### Preparation of polyurea coatings with modified melamine polyphosphate

After the fire-retardant polyurea samples were prepared in a beaker by mixing the FR additives in the diamine oligomer (Component B); a homogeneous mixture was obtained by using a high-speed mechanical stirrer. Then, diisocyanate was added to the beaker with vigorous stirring for 30 s, and the resultant mixture was poured into a 100 × 100 × 100 mm Teflon mold. In total, 15 g of each of Part A and B were to be prepared separately. The stoichiometric ratio of diisocyanate to diamine is 3:7<sup>13,14</sup>.

To achieve a better mixture, the mixture was placed in a Kakuhunter SK-300TVSII vacuum mixer (Shashin Kagaku Pte Ltd., Kyoto, Japan) for 180 s. During the mixing, a vacuum level of 0.5 kPa was kept to remove bubbles in the product. The revolution and rotation speed were set as 580 rpm and 1700 rpm, respectively. The mixer was a revolution-rotation mixer with a vacuum level of 0.1 kPa. The maximum revolution speed and rotation speeds are 1700 rpm and 1160 rpm, respectively. The bubble burst effect would be induced by the revolution-rotation design under a vacuum. All samples were cured at room temperature for 12 h and then were kept in an oven at 333 K for 24 h to complete the curing<sup>13–15</sup>. Additives and inorganic fillers examined could be found in Supplementary Table 2. The control groups with matrix only were named according to the previous matrix code as CS1 to CS4, whereas the AR3 and AR4 matrix groups with TiO<sub>2</sub>, TiO<sub>2</sub> and MPP, and Talc and MPP additives were named as ES5 and ES6; ES7 and ES8; ES9 and ES10 respectively.

### Fourier transform infrared (FTIR) spectroscopy

The presence of chemical reactions between basic polyurea and fire-retardant polyurea was determined by FTIR spectroscopy (Perkin Elmer Spectrum GX, Tokyo, Japan) scanned in the mid-infrared region set to the following parameters: range = 4000–600 cm<sup>-1</sup>, number of scans = 8<sup>15</sup>.

### Transmission Electron Microscopy (TEM)

Morphology of the basic polyurea and fire-retardant polyurea were observed via transmission electron microscopy (TEM) using a JEOL JEM 3010 (300 kV) (JSM-6510-LV, JEOL, Tokyo, Japan) microscope. The samples were diluted with distilled water and stained with 2% phosphotungstic acid solution<sup>15</sup>.

### Physico-mechanical properties

Instron 5500 R mechanical test machine with a 30 kN load cell was used to conduct a tensile test. The polyurea coating specimen was cut to size according to the ASTM-D638 standard. To ensure the test was a quasi-static process, the strain rate of the tensile test was set as low as 6 × 10<sup>-4</sup> s<sup>-1</sup>. A cylindrical cutter with a 6 mm inner diameter compressed with the hydronic compressor was used to prepare specimens for compression tests of the yield stress. The hardness of the polyurea sheet was tested with Teclock GS-709 N durometer type-A according to ASTM-D-2240. Measurements were acquired five times for each sample to get the average value with a short contact time of 1.0 s<sup>15,23,24</sup>.

### Differential scanning calorimetry (DSC) analysis

The maximum degradation temperature ( $T_{max}$ ) and thermal phase behavior of fire-retardant polyurea was determined by DSC TA Q10 (New Castle, USA) differential scanning calorimetry (DSC) by TA instruments, under nitrogen (gas flow of 50 ml/min) at a heating rate of 10 °C/min to 250 °C. Typical sample weights of 5–10 mg were employed. All coating samples were run in duplicates, and the average values are recorded. An empty aluminum pan was used as a reference. Before the start of the experiment, the temperature was equilibrated to 50 °C<sup>16</sup>.

### Burning analysis/flammability test

The equipment for the flammability test was horizontal burning type and the dimension was in accordance with ASTM D635<sup>17</sup>. Equipment consisted of a lighter and a stopwatch. The lighter's flame was used to ignite the specimen for flammability. The specimen was marked into three columns, the column from the right side was the area where the flame is passed to cover a 100 mm distance and the time was noted using a stopwatch. The flame should be extinguished at the center of the specimen when it passed the first 25 mm. The dimension for the sample given as per ASTM was 100 × 10 × 2 mm. The sample was exposed to flame for 10.0 s using Bunsen burner<sup>17,18</sup>. The final test was mainly concerned with the flammability test done on aromatic-substituted polyurea and flame-retardant aromatic-substituted polyurea to infer the difference between the two tests and to observe and conclude the beneficial presence of flame-resistant fillers and additives to polyurea.

### Scanning electron microscopy (SEM) imaging

The morphology of the burnt specimen was also obtained at different time intervals by scanning electron microscopy (SEM) using Hitachi S-4700 (California, CA, USA)<sup>13–15</sup>.

### DATA AVAILABILITY

The data that support the findings of this study are available from the corresponding author upon reasonable request.

Received: 24 January 2022; Accepted: 10 April 2022;

Published online: 02 May 2022

### REFERENCES

- Li, Y., Liu, Y., Yao, B., Narasimalu, S. & Dong, Z. Rapid preparation and anti-microbial activity of polyurea coatings with RE-doped nano-ZnO. *Microb. Biotechnol.* **15**, 548–560 (2022).
- Mariappan, T. & Wilkie, C. Thermal and fire-retardant properties of polyurea. *Polimery* **58**, 371–384 (2013).
- Hinnant, K. M., Giles, S. L., Smith, E. P., Snow, A. W. & Ananth, R. Characterizing the role of fluorocarbon and hydrocarbon surfactants in firefighting-foam formulations for fire-suppression. *Fire Technol.* **56**, 1413–1441 (2020).
- Li, Y., Woo, Y., Sekar, M., Narasimalu, S. & Dong, Z. Effect of nano-titanium dioxide contained in titania-polyurea coating on marina biofouling and drag reduction. *J. Biomed. Nanotechnol.* **15**, 1530–1541 (2020).
- Underhill, R., DiLoreto, S. & DiLoreto, B. Development of polyureas with improved fire resistance. *J. Fire Sci.* **31**(3), 211–226 (2012).
- Ma, Y., Dang, X. & Shan, Z. Thermal analysis and identification of potential fire-proof energy building material based on artificial leather. *J. Therm. Sci.* **28**, 88–96 (2019).
- Ovchinnikov, V. A. & Yakimov, A. S. Modeling of the thermal protection of a multilayer material under fire conditions. *J. Eng. Phys. Thermophys.* **89**, 569–578 (2016).
- Thirumal, M., Khastgir, D., Nando, G., Naik, Y. & Singha, N. Halogen-free flame retardant PUF: effect of melamine compounds on mechanical, thermal and flame retardant properties. *Polym. Degrad. Stab.* **95**, 1138–1145 (2010).
- van der Veen, I. & de Boer, J. Phosphorus flame retardants: properties, production, environmental occurrence, toxicity and analysis. *Chemosphere* **88**, 1119–1153 (2012).
- Yang, Y. et al. Flame retarded rigid polyurethane foam composites based on gel-silica microencapsulated ammonium polyphosphate. *J. Sol. Gel Sci. Technol.* **98**, 212–223 (2021).
- Bich, N. Thuy, effects of additives, pigment and filler on physico-mechanical properties and weather resistance of polyurea coatings. *Vietnam J. Sci. Technol.* **55**, 153 (2018).
- Zhao, W., Cheng, Y., Li, Z., Li, X. & Zhang, Z. Improvement in fire-retardant properties of polypropylene filled with intumescent flame retardants, using flower-like nickel cobaltate as synergist. *J. Mater. Sci.* **56**, 2702–2716 (2021).
- Li, Y., Luo, B., Guet, C., Narasimalu, S. & Dong, Z. Preparation and formula analysis of anti-biofouling titania-polyurea spray coating with nano/micro-structure. *Coatings* **9**, 560 (2019).
- Li, Y., Peng, X., Wang, Y. & Hao, Y. Mechanisms and control measures of mature biofilm resistance to antimicrobial agents in the clinical context. *ACS Omega* **5**, 22684–22690 (2020).
- Yang, J. Y. et al. Flame-retardant and self-healing biomass aerogels based on electrostatic assembly. *Chin. J. Polym. Sci.* **38**, 1294–1304 (2020).



16. Ortelli, S., Malucelli, G., Blosi, M., Zanoni, I. & Costa, A. L. AL, nanoTiO<sub>2</sub>@DNA complex: a novel eco, durable, fire retardant design strategy for cotton textiles. *J. Colloid Interface Sci.* **546**, 174–183 (2019).
17. Manfredi, A., Carosio, F., Ferruti, P., Ranucci, E. & Alongi, J. Linear poly-amidamines as novel biocompatible phosphorus-free surface-confined intumescent flame retardants for cotton fabrics. *Polym. Degrad. Stab.* **151**, 52–64 (2016).
18. Zaman, Q. et al. A comprehensive review on synthesis, characterization, and applications of polydimethylsiloxane and copolymers. *Int. J. Plast. Technol.* **23**, 261–282 (2019).
19. Zhang, S. et al. The novel application of chitosan: effects of cross-linked chitosan on the fire performance of thermoplastic polyurethane. *Carbohydr. Polym.* **189**, 313–321 (2018).
20. McKenna, H. "The fire toxicity of polyurethane foams". *Fire Sci. Rev.* **5**, 3 (2016).
21. Wu, Q. & Qu, B. Synergistic effects of silicotungstic acid on intumescent flame-retardant polypropylene. *Polym. Degrad. Stab.* **74**, 225–261 (2001).
22. Daimatsu, K. et al. Preparation and physical properties of flame retardant acrylic resin containing nano-sized aluminum hydroxide. *Polym. Degrad. Stab.* **92**, 1433–1438 (2007).
23. Nguyen, T. N., Trinh, H. T., Sam, L. H., Nguyen, T. Q. & Le, G. T. Halogen-free flame-retardant flexible polyurethane for textile coating: preparation and characterisation. *Fire Mater.* **44**, 269–282 (2020).
24. Ortelli, S. et al. Coatings made of proteins adsorbed on TiO<sub>2</sub> nanoparticles: a new flame retardant approach for cotton fabrics. *Cellulose* **25**, 2755–2765 (2018).

## ACKNOWLEDGEMENTS

This research was funded by MOE Academic Research Fund (AcRF) Tier 1 Project "Nano-structured Titania with tunable hydrophilic/hydrophobic behavior and photocatalytic function for marine structure application", Grant Call (Call 1/2018)\_MSE (EP Code EP5P, Project ID 122018-T1-001-077), Ministry of Education (MOE), Singapore.

## AUTHOR CONTRIBUTIONS

Z.R. and Y.L. make substantial contributions to the conception and design of the work and the acquisition; R.Z.L. and H.W. greatly contribute to the analysis and interpretation of the data; Z.R. and R.Z.L. draft the work; Y.L. and X.W. revise it critically for important intellectual content; Y.L. makes the final approval of the

completed version; Z.R. and Y.L. take the accountability for all aspects of the work in ensuring that questions related to the accuracy or integrity of any part of the work are appropriately investigated and resolved; K.L. is in charge of visualization of the figures and diagrams as well as formatting of the work.

## COMPETING INTERESTS

The authors declare no competing interests.

## ADDITIONAL INFORMATION

**Supplementary information** The online version contains supplementary material available at <https://doi.org/10.1038/s41529-022-00248-y>.

**Correspondence** and requests for materials should be addressed to Yuanzhe Li.

**Reprints and permission information** is available at <http://www.nature.com/reprints>

**Publisher's note** Springer Nature remains neutral with regard to jurisdictional claims in published maps and institutional affiliations.



**Open Access** This article is licensed under a Creative Commons Attribution 4.0 International License, which permits use, sharing, adaptation, distribution and reproduction in any medium or format, as long as you give appropriate credit to the original author(s) and the source, provide a link to the Creative Commons license, and indicate if changes were made. The images or other third party material in this article are included in the article's Creative Commons license, unless indicated otherwise in a credit line to the material. If material is not included in the article's Creative Commons license and your intended use is not permitted by statutory regulation or exceeds the permitted use, you will need to obtain permission directly from the copyright holder. To view a copy of this license, visit <http://creativecommons.org/licenses/by/4.0/>.

© The Author(s) 2022